Inorg. Chem. **2008**, *47*, 10953−10958

Effect of Charge and Composition on the Structural Fluxionality and Stability of Nine Atom Tin−Bismuth Zintl Analogues

Ujjwal Gupta,[†] Arthur C. Reber,[‡] Penee A. Clayborne,[‡] Joshua J. Melko,[†] Shiv N. Khanna,[‡] and A. W. Castleman, Jr.*[,†]

Department of Chemistry and Physics, The Pennsylvania State University, University Park, Pennsylvania 16802, and Department of Physics, Virginia Commonwealth University, Richmond, Virginia 23220

Received June 24, 2008

Synergistic studies of bismuth doped tin clusters combining photoelectron spectra with first principles theoretical investigations establish that highly charged Zintl ions, observed in the condensed phase, can be stabilized as isolated gas phase clusters through atomic substitution that preserves the overall electron count but reduces the net charge and thereby avoids instability because of coulomb repulsion. Mass spectrometry studies reveal that Sn_8Bi^-, $Sn_7Bi_2^-$, and $Sn_6Bi_3^-$ exhibit higher abundances than neighboring species, and photoelectron spectroscopy show that all of these heteroatomic gas phase Zintl analogues (GPZAs) have high adiabatic electron detachment energies. $Sn_6Bi_3^-$ is found to be a particularly stable cluster, having a large highest occupied molecular orbital (HOMO)−lowest unoccupied molecular orbital (LUMO) gap. Theoretical calculations demonstrate that the $Sn_6Bi_3^-$ cluster is isoelectronic with the well know Sn_9^{-4} Zintl ion; however, the fluxionality reported for Sn_9^{-4} is suppressed by substituting Sn atoms with Bi atoms. Thus, while the electronic stability of the clusters is dominated by electron count, the size and position of the atoms affects the dynamics of the cluster as well. Substitution with Bi enlarges the cage compared with Sn_9^{-4} making it favorable for endohedral doping, findings which suggest that these cages may find use for building blocks of cluster assembled materials.

Introduction

Ever since their discovery in 1930, stable polyatomic anions of the post transition metal and semimetal atoms have drawn considerable interest.[1−4] These anions, called Zintl ions, are fairly stable and combine with cations to form solids or melts called Zintl phases. Studies of their structure and exploration of their stability has remained an active subject of investigation.[1−11] Since Zintl ions are well-known in the condensed phase, there has been interest in examining their stability and properties as free ions in the gas phase.[12−17] This renewed interest is partly driven by the recent quest in developing cluster assembled materials where size selected atomic clusters serve as the primitive building blocks.[18−23] As the properties of clusters can be altered by size and

* To whom correspondence should be addressed. E-mail: awc@psu.edu.
† The Pennsylvania State University.
‡ Virginia Commonwealth University.

(1) Corbett, J. D. *Chem. Rev.* **1985**, *85*, 383–397.
(2) Corbett, J. D. Diverse naked clusters of the heavy main-group elements. Electronic regularities and analogies. In *Structural And Electronic Paradigms In Cluster Chemistry*; Springer-Verlag: New York, 1997; Vol. *87*, pp 157−193.
(3) Corbett, J. D. *Angew. Chem., Int. Ed.* **2000**, *39*, 670. -+
(4) Sevov, S. C.; Goicoechea, J. M. *Organometallics* **2006**, *25*, 5678–5692.
(5) King, R. B.; Silaghi-Dumitrescu, I. *Inorg. Chem.* **2003**, *42*, 6701–6708.
(6) King, R. B.; Silaghi-Dumitrescu, I.; Lupan, A. *Dalton Trans.* **2005**, 1858–1864.
(7) King, R. B.; Silaghi-Dumitrescu, I.; Lupan, A. *Inorg. Chem.* **2005**, *44*, 3579–3588.
(8) King, R. B.; Silaghi-Dumitrescu, I.; Uta, M. M. *Inorg. Chem.* **2006**, *45*, 4974–4981.
(9) Queneau, V.; Sevov, S. C. *J. Am. Chem. Soc.* **1997**, *119*, 8109–8110.
(10) Sevov, S. C.; Goicoechea, J. M. *Chem. Abstr.* **2005**, *230*, U2037–U2037.
(11) Ugrinov, A.; Sen, A.; Reber, A. C.; Qian, M.; Khanna, S. N. *J. Am. Chem. Soc.* **2008**, *130*, 782–783.
(12) Farley, R. W.; Castleman, A. W., Jr. *J. Chem. Phys.* **1990**, *92*, 1790–1795.
(13) Farley, R. W.; Ziemann, P.; Castleman, A. W., Jr. *Z. Physik D: At., Mol. Clusters* **1989**, *14*, 353–360.
(14) Farley, R. W.; Castleman, A. W., Jr. *J. Am. Chem. Soc.* **1989**, *111* (7), 2734–2735.
(15) Wheeler, R. G.; LaiHing, K.; Wilson, W. L.; Duncan, M. A. *J. Chem. Phys.* **1988**, *88*, 2831–2839.
(16) LaiHing, K.; Cheng, P. Y.; Duncan, M. A. *J. Phys. Chem.* **1987**, *91: 26*, 6521–6525.
(17) Wheeler, R. G.; LaiHing, K.; Wilson, W. L.; Allen, J. D.; King, R. B.; Duncan, M. A. *J. Am. Chem. Soc.* **1986**, *108*, 8101–8102.

10.1021/ic8011712 CCC: $40.75
Published on Web 10/25/2008

composition, the feasibility of cluster assembled materials would provide a novel approach to synthesizing materials with tunable properties. Studies of Zintl ions in the gas phase could provide information on how stable clusters in beams can be translated into developing condensed phase cluster materials and reveal unique structures and properties such as those associated with the Stannaspherene cluster.[24,25] Two prominent Zintl anions in this category are Sn_9^{-2} and Sn_9^{-4}.[5,26,27] The Sn_9^{-2} species with 20 electrons has a closo D_{3h} structure, which can be accounted for within Wade−Mingos rules.[28−31] The other stable cluster is the Sn_9^{-4} anion. Previous theoretical studies have indicated that the Sn_9^{-4} cluster has a square-antiprismatic ground state and represents a nido-type cluster.[5] Sn_9^{-4} is isoelectronic with the Bi_9^{+5} cluster, whose electronic structure was determined in a pioneering study by Corbett and Rundle.[32] Its stability is also explained by Wade−Mingos rules. According to these rules, a closo (D_{3h}) cluster with n vertices exhibits enhanced stability for $2n + 2$ electrons while a nido (C_{4v}) cluster with n vertices exhibits enhanced stability for 2n+4 electrons. Since each Sn atom contributes two p-electrons to the valence pool, the stability of Sn_9^{-2} and Sn_9^{-4} with 20 and 22 valence electrons, respectively, can be reconciled within such a simple model. In addition to the nido-C_{4v} structure, the Sn_9^{-4} cluster is found to exhibit a closely lying isomer with a closo-D_{3h} structure. This gives the cluster some structural fluxionality, as the breaking or stretching of one bond in the D_{3h} geometry can lead to the C_{4v} structure. Such fluxionality is also shown by the Zintl anions Ge_9^{-4} and Pb_9^{-4}, and all these clusters are marked by 22 valence p-electrons.[5,26] Since a cluster's electronic structure is intimately linked to its geometrical configuration, the existence of isomers must relate to special electronic features at 22 electrons that override the changes in geometry and atomic size.

The above observations raise important questions regarding the relationship between geometry and the electron count. If the existence of the isomers is dependent on the number of electrons, it is of interest to explore how their relative stability evolves as the charge on the anion is progressively altered while the electron count is kept constant. This can be accomplished by replacing some of the Sn atoms with Bi atoms, which would contribute one additional electron each.[33−35] The extra electron from the substituted Bi atom should decrease by one the overall charge for the most stable anion for each substitution. Will the isomeric behavior continue to take place, and if so what effect does this substitution have on the relative stability of the two isomers? Furthermore, what role do the sizes of the constituent atoms play as one substitute a larger Bi atom in place of a Sn atom? The purpose of this paper is to answer the above questions through studies of Sn_9^{-q} ($q = 1-4$) and $Sn_{9-x}Bi_x^-$ ($x = 1-3$), free clusters, where the number of atoms and the charged state can be varied one atom and one electron at a time. The present paper represents a synergistic effort where first principles electronic structure calculations are combined with results from negative ion photoelectron spectroscopy experiments to ascertain the electronic structure of the systems. We show that while in Sn_9^{-4} clusters, the C_{4v} and D_{3h} isomers have comparable stability, the bismuth doped analogue, $Sn_6Bi_3^-$, shows a marked preference toward the D_{3h} isomer (0.22 eV lower in energy). Through studies of $Sn_{9-x}Bi_x$ clusters containing 1−3 Bi atoms, we demonstrate that the geometrical size also contributes to the structural fluxionality and that the fluxional conversion can be suppressed by substituting Sn atoms with Bi atoms. Further, the $Sn_6Bi_3^-$ cluster shows unique stability, and the reasons for this are explored through molecular orbital diagrams and aromaticity studies.

Experimental Method

The electronic structure of the anions was probed via negative ion photoelectron spectroscopy. A beam of mass selected anions is crossed with a photon beam to analyze the kinetic energies of the photodetached electrons. If hv is the energy of the photon and e^-KE is the measured kinetic energy of the emitted electron, the difference (hv − e^-KE) provides a direct measure of the energy required to make a transition from the anion of multiplicity M to neutral clusters with multiplicity M ± 1. As the transition to the neutral cluster can occur to the ground or excited states of the multiplicity M ± 1, the photodetachment spectra provides a fingerprint of the electronic structure for comparison with the theoretical calculations. When the calculated transitions agree with experiment, it can reasonably be assumed that the calculated ground state including its multiplicity should be correct. The experimental investigations focused on $Sn_{9-x}Bi_x^-$ clusters.

The details of the apparatus employed in this study have been described elsewhere.[36] In brief, $Sn_xBi_y^-$ clusters were formed by using a 1/4" 50:50 molar ratio Sn−Bi molded rod in a laser vaporization source. Helium was used as a carrier gas, and the clusters were mass analyzed using Wiley−McLaren time-of-flight mass spectrometry.[37] The photoelectron spectra for the clusters were

(18) Bergeron, D. E.; Roach, P. J.; Castleman, A. W., Jr.; Jones, N.; Khanna, S. N. *Science* **2005**, *307*, 231–235.
(19) Castleman, A. W., Jr.; Khanna, S. N.; Sen, A.; Reber, A. C.; Qian, M.; Davis, K. M.; Peppernick, S. J.; Ugrinov, A.; Merritt, M. D. *Nano Letters* **2007**, *7*, 2734–2741.
(20) Roach, P. J.; Reber, A. C.; Woodward, W. H.; Khanna, S. N.; Castleman, A. W., Jr. *Proc. Natl. Acad. Sci. U.S.A.* **2007**, *104*, 14565–14569.
(21) Jadzinsky, P. D.; Calero, G.; Ackerson, C. J.; Bushnell, D. A.; Kornberg, R. D. *Science* **2007**, *318*, 430–433.
(22) Reber, A. C.; Khanna, S. N.; Castleman, A. W., Jr. *J. Am. Chem. Soc.* **2007**, *129*, 10189–10194.
(23) Khanna, S. N.; Jena, P. *Phys. Rev. B* **1995**, *51*, 13705.
(24) Cui, L. F.; Huang, X.; Wang, L. M.; Zubarev, D. Y.; Boldyrev, A. I.; Li, J.; Wang, L. S. *J. Am. Chem. Soc.* **2006**, *128*, 8390–8391.
(25) Cui, L. F.; Huang, X.; Wang, L. M.; Li, J.; Wang, L. S. *Angew. Chem., Int. Ed.* **2007**, *46*, 742–745.
(26) Queneau, V.; Sevov, S. C. *Inorg. Chem.* **1998**, *37*, 1358–1360.
(27) Hirsch, A.; Chen, Z. F.; Jiao, H. J. *Angew. Chem., Int. Ed.* **2001**, *40*, 2834–2838.
(28) Wade, K. *J. Chem. Soc., Chem. Commun.* **1971**, 792.
(29) Wade, K. *Inorg. Nucl. Chem. Lett.* **1972**, *8*, 559.
(30) Mingos, D. M. P. *J. Chem. Soc., Chem. Commun.* **1983**, 706–708.
(31) Mingos, D. M. P. *Acc. Chem. Res.* **1984**, *17*, 311–319.
(32) Corbett, J. D.; Rundle, R. E. *Inorg. Chem.* **1964**, *3*, 1408–1412.
(33) Sun, S. T.; Liu, H. T.; Tang, Z. C. *J. Phys. Chem. A* **2006**, *110*, 5004–5009.
(34) Andreas Hartmann, K. G. W. *Angew. Chem., Int. Ed. Engl.* **1988**, *27*, 1091–1092.
(35) Xu, L.; Sevov, S. C. *Inorg. Chem.* **2000**, *39*, 5383–5389.
(36) Knappenberger, K. L.; Jones, C. E.; Sobhy, M. A.; Castleman, A. W., Jr. *Rev. Sci. Instrum.* **2006**, 77.
(37) Wiley, W. C.; McLaren, I. H. *Rev. Sci. Instrum.* **1955**, *26*, 1150–1157.

obtained using a magnetic bottle time-of-flight photoelectron spectrometer[38] and employing photons from a 308 nm excimer laser for electron detachment.

Theoretical Method

The theoretical investigations were carried out within a density functional formalism[39,40] that incorporated exchange and correlation effects within the generalized gradient approximation (GGA) functional proposed by the gradient-corrected BP86 DFT functional.[41,42] The molecular structures of the studied species were optimized using a Quadruple-ζ with polarization functions (QZ4P) basis set with an all electron calculation. The Zeroth-Order Regular Approximation (ZORA) was employed in the calculation to account for the scalar relativistic effects.[43] Excited states were calculated using time-dependent DFT (TDDFT).

For each cluster size, the geometry was optimized by starting from several initial configurations and moving the atoms along the direction of forces until the forces dropped below a threshold value. The present studies involve comparison with negative ion photoelectron spectra, and we have used the following approach to compute the theoretical spectra. First, we studied the vertical transition from the anion to the neutral species where the neutral cluster has the same geometry as the anion. For example, starting from the anion cluster with a spin multiplicity of M, the energies of the neutral clusters with multiplicities M ± 1 were calculated. Since the photodetachment processes are fast compared to the time for relaxing atomic structure, the difference in energy can be compared with the peaks in the photoelectron spectra. Then, higher energy peaks were calculated using excited states of the neutral at the anion geometry. The electronic structure was checked to ensure that the hole is consistent with ejecting a single electron from the anion structure, and then allowing the electronic structure to relax. We also calculated the adiabatic electron affinities that correspond to the difference in energy between the ground state of the anion and neutral species to make comparisons with experiments where such information was available.

Results

We first investigated the effect of charge on the fluxional behavior of the Sn_9^{-q} ($q = 1-4$) clusters into the D_{3h} and C_{4v} isomers. The results on the lowest energy structures (within the symmetry constraint) and their relative stability are shown in Figure 1. Note that the D_{3h} structure is more stable in Sn_9^-, Sn_9^{-2}, and Sn_9^{-3}. However, for Sn_9^{-4} the D_{3h} structure differs from the C_{4v} structure by only 0.003 eV, which is beyond the accuracy of the calculations, and hence, the two structures are considered degenerate. Previous studies have shown that the polyatomic anion Sn_9^{-4} in the condensed phase exhibits D_{3h} and C_{4v} structures that can interconvert.[44,45] To further examine the fluxional behavior in this

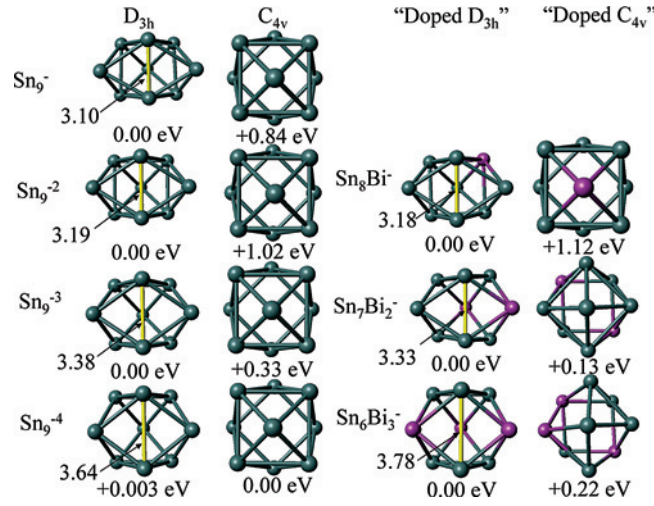

Figure 1. Geometry and relative energy of Sn_9^{-x} clusters with D_{3h} and C_{4v} geometries, and the relative energies in their isoelectronic $Sn_nBi_y^-$ clusters.

species, we calculated the barrier for the transition from the D_{3h} ground state to the C_{4v} structure by calculating the total energy for various values of the diagonal Sn−Sn bond length in the square. The barrier was less than 0.01 eV! This shows that the interconversion could occur under normal conditions of temperature. However, this is not the case for the other Sn_9 anions. The charge has a major effect on the fluxional behavior of the cluster. As shown in Figure 1, when the charge is reduced from −4 to −3, the C_{4v} structure is destabilized by about 0.33 eV relative to the D_{3h} structure. Further, as the charge is reduced from −2 to −1, the C_{4v} structure is destabilized by 0.18 eV compared to the D_{3h} structure. As expected, the D_{3h} structure for Sn_9^{-2} is much more stable, 1.02 eV lower in energy, a result of Wade−Mingos rules discussed in the introduction.

While the multiply charged clusters are observed in the condensed phase, the coulomb repulsion destabilizes the binding of multiple electrons in free clusters. Consequently, a different approach has to be utilized. One way is to replace some of the Sn atoms with Bi atoms. As a Bi atom has one more valence electron than Sn, it should be possible to create singly charged species having the same number of electrons as in Sn_9^{-q}. In this work, $Sn_6Bi_3^-$, $Sn_7Bi_2^-$, and Sn_8Bi^- have the same number of electrons as Sn_9^{-4}, Sn_9^{-3}, and Sn_9^{-2}, respectively, and hence one can find information through the use of these mixed anions. It is important to underscore that the size of a Bi atom is larger than that of a Sn atom. Hence, while the replacement of Sn by Bi enables one to control the overall charge, the substitution of Sn by Bi also involves the effect of size. As we show, the difference in size does slightly reduce the overall stability.

We first studied the relative stability of the D_{3h} and C_{4v} structures in $Sn_6Bi_3^-$, $Sn_7Bi_2^-$, and Sn_8Bi^- clusters, shown in Figure 1. Note that, in all cases, the ground state has a D_{3h} structure as in the case of Sn_9^{-q} clusters. The replacement of the Sn atom with Bi breaks the symmetry, and we use D_{3h} to indicate closo geometries and C_{4v} to indicate nido geometries. For Sn_8Bi^- which is the analogue of Sn_9^{-2}, the D_{3h} is indeed more stable than the C_{4v} structure by 1.12 eV,

(38) Kruit, P.; Read, F. H. *J. Phys. E: Sci. Instrum.* **1983**, *16*, 313–324.
(39) Kohn, W.; Sham, L. J. *Phys. Rev.* **1965**, *140*, 1133.
(40) G te Velde, F. M. B.; Baerends, E. J.; Fonseca Guerra, C.; van Gisbergen, S. J. A.; Snijders, J. G.; Ziegler, T. *J. Comput. Chem.* **2001**, *22*, 931–967.
(41) Becke, A. D. *Phys. Rev. A* **1988**, *38*, 3098.
(42) Perdew, J. P. *Phys. Rev. B* **1986**, *33*, 8822.
(43) Fonseca Guerra, C.; Snijders, J. G.; te Velde, G.; Baerends, E. J. *Theor. Chem. Acc.* **1998**, *99*, 391–403.
(44) Rudolph, R. W.; Wilson, W. L.; Parker, F.; Taylor, R. C.; Young, D. C. *J. Am. Chem. Soc.* **1978**, *100*, 4629–4630.
(45) Rudolph, R. W.; Wilson, W. L.; Taylor, R. C. *J. Am. Chem. Soc.* **1981**, *103*, 2480–2481.

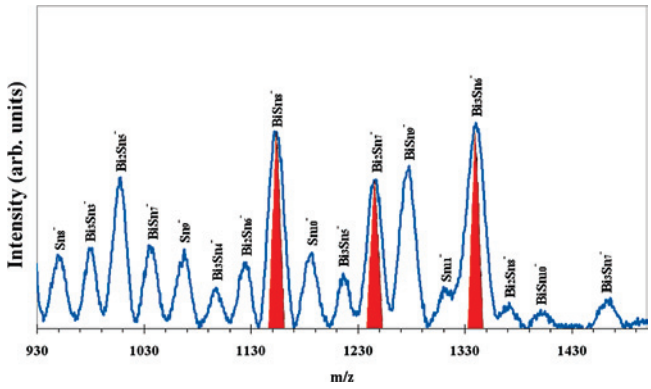

Figure 2. Experimental Mass Spectrum of $Sn_xBi_y^-$ clusters.

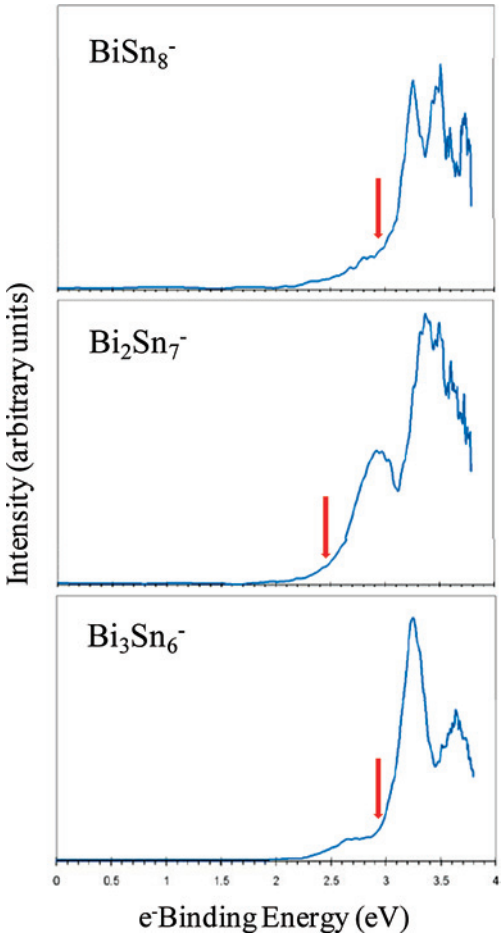

Figure 3. Photoelectron spectra of 9 atom Tin−Bismuth Zintl analogues.

comparable to 1.02 eV in Sn_9^{-2}. For $Sn_7Bi_2^-$, the structure C_{4v} converted to D_{3h}, and the C_{4v} structure was found to be 0.13 eV less stable. Finally, for $Sn_6Bi_3^-$ the two structures differ by only 0.22 eV, compared to 1.12 eV for Sn_8Bi^-. This shows that while the trend toward fluxionality in pure Sn_9^{-q} clusters, as q increases, is maintained, the differing size of Bi and Sn in $Sn_6Bi_3^-$ does result in the C_{4v} structure lying higher in energy by 0.22 eV. Thus, while the behavior is dominated by electron count, the size of the atoms changes the relative stability of the isomers of different symmetry.

These findings were substantiated through an experimental study of the $Sn_6Bi_3^-$, $Sn_7Bi_2^-$, and Sn_8Bi^- clusters. Figure 2 shows the mass spectrum of the anions produced from ablation of a Sn−Bi rod. The spectrum shows that all the 9 atom clusters ($Sn_6Bi_3^-$, $Sn_7Bi_2^-$, and Sn_8Bi^-) appear with appreciable intensity compared to their neighboring species and hence are quite stable. To investigate the electronic features of these stable species, negative ion photoelectron spectra were taken and are shown in Figure 3. Assigned values of spectral features are presented in Table 1. The adiabatic electron detachment energy (AEDE) corresponds to the difference in energy between the ground state of the anion and the ground state of the neutral species. The experimental assignment is derived by linear extrapolation of the onset marking the first peak. Additional information on the anion geometry is provided by the peaks of the features in the photodetachment spectra that correspond to vertical transitions from the anion with a multiplicity (M) to neutral clusters with multiplicity M ± 1. These vertical detachment energies (VDEs) are also listed in Table 1.

Accompanying these experimentally determined values are the theoretical assignments of AEDE and VDE provided by first principles electronic structure calculations. Table 1 shows the calculated adiabatic electron detachment energies and vertical detachment energies for the Sn_9^-, $Sn_6Bi_3^-$, $Sn_7Bi_2^-$, and Sn_8Bi^- clusters undergoing a transition from an anion to a neutral with multiplicity M ± 1. To examine cluster stability, we also calculated the energy required to remove a Sn or a Bi atom from the cluster, listed as ΔE_{Sn} and ΔE_{Bi}. Also shown in Table 1 are the Removal Energies (R.E.) calculated using the equation

$$\text{R.E.(Sn)} = E(Sn_{x-1}Bi_y^-) + E(Sn) - E(Sn_xBi_y^-) \qquad (1)$$

Here E(Sn) is the total energy of a Sn atom, $E(Sn_xBi_y^-)$ is the total energy of the $Sn_xBi_y^-$ cluster, and $E(Sn_{x-1}Bi_y^-)$ is the total energy of the cluster with one fewer Sn atom. A similar calculation is done to determine the Bi removal energy. We also calculated the gap between the highest occupied molecular orbital (HOMO) and the lowest unoccupied molecular orbital (LUMO) for the anion. These are also listed in Table 1. A large HOMO−LUMO gap is a signature of electronic stability and reduced chemical reactivity as the cluster prefers to neither donate nor to receive another electron.[46,47]

Table 1. Experimental and Theoretical Values for the $Sn_xBi_y^-$ Clusters[a]

	experimental			theoretical						
cluster	VDE	VDE2	AEDE	VDE	VDE2	AEDE	Gap	Sn R.E.	Bi R.E.	Bi Exc.
Sn_8Bi^-	3.26 ± 0.02	3.47 ± 0.05	2.95 ± 0.07	3.11	3.19	2.97	1.18	3.64	3.47	0.09
$Sn_7Bi_2^-$	2.93 ± 0.07	3.40 ± 0.07	2.47 ± 0.11	2.72	3.27	2.26	0.21	3.43	3.10	−0.52
$Sn_6Bi_3^-$	3.25 ± 0.04	3.63 ± 0.05	2.96 ± 0.06	3.04	3.61	2.92	2.25	3.60	3.51	0.07

[a] All values are in eV.

The first thing to note in Table 1 is that the calculated values of AEDE and VDE are in good agreement with experiment. As mentioned before, the vertical transitions provide a fingerprint of the geometrical structure, and the close agreement shows that the calculated structures match with experiment. As expected, the AEDE is higher for the Sn_8Bi^- and $Sn_6Bi_3^-$ clusters, as they are the Sn_9^{-2} and Sn_9^{-4} analogues and are particularly stable. This is also seen in the Sn R.E and Bi R.E values, which show larger values for Sn_8Bi^- and $Sn_6Bi_3^-$. The Bi exchange energy, which is a comparison of the atomization energies, has also been calculated. This shows that the doping with a Bi atom in Sn_8Bi^- and $Sn_6Bi_3^-$ increases the stability, while it decreases the stability in $Sn_7Bi_2^-$.

$$\text{Bi Exc.}(Sn_xBi_y^-) = E(Sn_{x+1}Bi_{y-1}^-) - E(Sn_xBi_y^-) \qquad (2)$$

The $Sn_6Bi_3^-$ cluster, in addition, exhibits a large HOMO−LUMO gap of 2.25 eV. As a point of reference, the HOMO−LUMO gap in the C_{60} cluster is around 1.70 eV,[48] and Al_{13}^- has a gap of 1.87 eV.[49]

While the substitution of Sn by Bi allows one to generate isoelectronic structures, the size of Bi is larger than Sn and this can affect the overall stability. To examine these size effects, we carried out calculations on $Sn_nSb_m^-$ clusters as Sb has the same number of valence electrons as Bi, but is in the same row as Sn. A comparison of the atomization energies of the 9 atom clusters with the same number of Sb and Bi atoms revealed that the substitution pattern is the same in both clusters, and that the larger size of Bi reduces the binding energy by about 0.25 eV per substitution compared to Sb. It can be noted that the near mass degeneracy of Sn and Sb make the experimental study of $Sn_nSb_m^-$ clusters difficult.

To further investigate the special electronic features that contribute to the stability of Sn_9^{-2} and Sn_9^{-4}, we show in Figure 4 the one electron levels in Sn_9^{-2}, Sn_9^{-4} (C_{4v}), and $Sn_6Bi_3^-$. The electronic levels dominated by p-states are shown. The continuous lines represent the occupied states while the dashed lines represent the unfilled states. Noticeably, the p-orbitals normal to the cage can form π-orbitals which differ from the expected Wade−Mingos structures and may lead to a spherical aromaticity while the other orbitals form skeleton molecular orbitals. Spherical aromaticity refers to the shell closures in the particle on a sphere with $2(n+1)^2$ electrons as opposed to $4n+2$ electrons which result in a shell closure in a particle on a ring. To show this more explicitly, we have shown the charge density distribution in the most stable electronic orbital, which corresponds to an overall π-bonding orbital. The next orbitals are either σ or composed of a mixture of σ-like and π-like. For the case of Sn_9^{-2}, the manifold of the skeleton orbitals is separated by

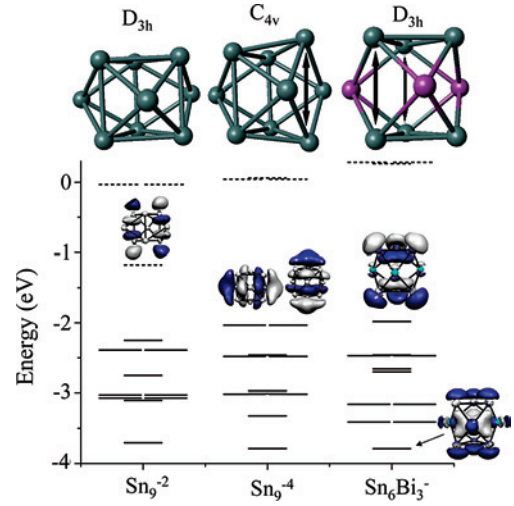

Figure 4. Electronic structure of the Sn_9^{-2}, Sn_9^{-4} C_{4v}, and $Sn_6Bi_3^-$. The levels of Sn_9^{-2} and Sn_9^{-4} have been shifted down by 3.54 and 8.75 eV, respectively, to that of $Sn_6Bi_3^-$. The charge density of the HOMO in Sn_9^{-4} has been plotted along with the analogous states in the other species, and the all π bonding orbital of $Sn_6Bi_3^-$.

the LUMO that has π-bonding in the top and bottom triangles leaving a node in the middle. Since the LUMO in Sn_9^{-2} is separated substantially from the LUMO+1, one can envision another stable species if the LUMO state could be filled by two additional electrons. In the pure Sn case, a distortion into C_{4v} or a simple stretching of the separation between two triangles in a D_{3h} structure stabilizes this LUMO and leads to another stable species in Sn_9^{-4}. The two distortions are shown in Figure 4. A C_{4v} distortion lowers the energy of the LUMO in Sn_9^{-2} and the cluster becomes stabilized by acquiring two extra electrons leading to Sn_9^{-4}. The addition of three Bi atoms to form $Sn_6Bi_3^-$ accomplishes a similar effect. As shown in Figure 4, the cluster exhibits a large HOMO−LUMO gap. To further examine the filling of the π-like orbitals, we calculated the Nucleus-Independent Chemical Shift (NICS) proposed by Schleyer and coworkers[50] that provides a magnetic criterion to identify the ring currents. Systems with negative NICS values have aromatic character while those with positive NICS values are considered antiaromatic. The calculated NICS values for Sn_8Bi^- and $Sn_6Bi_3^-$ were −33.4 and −37.7, respectively, both of which are large negative values and further confirm the presence of filled π orbitals.

To summarize, we have examined the fluxionality and stability of pure Sn_9^{-q} and mixed $Sn_{9-x}Bi_y^-$ clusters. The studies show a similar trend in fluxionality for both the pure and mixed systems but also reveal that atomic size does play a role in the relative stability. Negative ion photoelectron experiments coupled with theoretical investigations have shown the Sn_8Bi^- and $Sn_6Bi_3^-$ species to be stable, a result of their similarities to the known Zintl ions Sn_9^{-2} and Sn_9^{-4}. Further, $Sn_6Bi_3^-$ is an unusually stable cluster with a large HOMO−LUMO gap.

One of the objectives of the research is to identify clusters with interesting properties that are suitable for cluster

(46) Pearson, R. G. *Proc. Natl. Acad. Sci. U.S.A.* **1986**, *83*, 8440–8441.
(47) Reber, A. C.; Khanna, S. N.; Roach, P. J.; Woodward, W. H.; Castleman, A. W., Jr. *J. Am. Chem. Soc.* **2007**, *129*, 16098–16101.
(48) Wang, Y.; Holden, J. M.; Rao, A. M.; Lee, W.-T.; Bi, X. X.; Ren, S. L.; Lehman, G. W.; Hager, G. T.; Eklund, P. C. *Phys. Rev. B* **1992**, *45*, 14396.
(49) Bergeron, D. E.; Castleman, A. W., Jr.; Morisato, T.; Khanna, S. N. *Science* **2004**, *304*, 84–87.
(50) Chen, Z. F.; Wannere, C. S.; Corminboeuf, C.; Puchta, R.; Schleyer, P. V. *Chem. Rev.* **2005**, *105*, 3842–3888.

assembled materials. Along these lines, we theoretically examined the spin magnetic moment of cages containing Fe, Co, and Ni atoms, as the inclusion of three Bi sites in $Sn_6Bi_3^-$ enlarges the cage compared to Sn_9^{-4}. We found that the resulting endohedral species had large binding energies, and spin magnetic moments of 3 μ_B, 2 μ_B, and 1 μ_B, respectively, offering the possibility of synthesizing magnetic materials using the stable cages.[51−53] The doping of the tin clusters with bismuth may allow for the formation of endohedrally doped tin cages with larger electronic stability than the $M@Sn_{12}^{-2}$ based cages,[54] and permit doping of smaller tin cage clusters.[55,56] The cages may also be used as a possible cluster assembled material for solar energy conversion, much like Bi_2S_3 and SnO_2 in various nanostructures.[57] We are currently exploring these options in a synergistic experiment−theory effort.

Acknowledgment. The authors gratefully acknowledge support from U.S. Department of Energy Grant DE-FG02-02ER46009.

IC8011712

(51) Robles, R.; Khanna, S. N.; Castleman, A. W., Jr. *Phys. Rev. B* **2008**, *77*, 235441.
(52) Pradhan, K.; Sen, P.; Reveles, J. U.; Khanna, S. N. *Phys. Rev. B* **2008**, *77*, 095408.
(53) Reber, A. C.; Khanna, S. N.; Hunjan, J. S.; Beltran, M. R. *Chem. Phys. Lett.* **2006**, *428*, 376–380.
(54) Cui, L. F.; Wang, L. S. *Int. Rev. Phys. Chem.* **2008**, *27*, 139–166.
(55) Kumar, V.; Singh, A. K.; Kawazoe, Y. *Nano Lett.* **2004**, *4*, 677–681.
(56) Xia Zhang, G. L.; Xing, X.; Zhao, X.; Tang, Z.; Gao, Z. *Rapid Commun. Mass Spectrom.* **2001**, *15*, 2399–2403.
(57) Kamat, P. V. *J. Phys. Chem. C* **2007**, *111*, 2834–2860.